Stochastic Models for Strength of Wind Turbine Blades using Tests

Toft, Henrik Stensgaard; Sørensen, John Dalsgaard

Published in:
EWEC 2008 Conference Proceedings

Publication date:
2008

Document Version
Publisher's PDF, also known as Version of record

Stochastic Models for Strength of Wind Turbine Blades using Tests

Henrik Stensgaard Toft, *Aalborg University, Denmark, hst@civil.aau.dk, phone +45 9940 8583*
John Dalsgaard Sørensen, *Aalborg University and Risø National Laboratory, Denmark*

Abstract
The structural cost of wind turbine blades is dependent on the values of the partial safety factors which reflect the uncertainties in the design values, including statistical uncertainty from a limited number of tests. This paper presents a probabilistic model for ultimate and fatigue strength of wind turbine blades especially considering the influence of prior knowledge and test results and how partial safety factors can be updated when additional full-scale tests are performed. This updating is performed by adopting a probabilistic design basis based on Bayesian statistical methods.

1. Introduction
To verify the ultimate and fatigue strength of new wind turbine blades, full-scale certification type tests must be performed according to [1]. Normally, several tests are performed with small coupons of the base material and a limited number of tests are performed with elements and details of the blade. However, normally only one full-scale test is performed according to the requirements in [2] which normally does not lead to failure. Only one non destructive full-scale test leaves a considerable amount of statistical uncertainty which must be taken into account in the assessment of the reliability and partial safety factors for the blades.

Blade testing in ultimate loading is normally performed by multiple-loading in about six locations on the blade dependent on the blade length. In fatigue loading the test load is often applied by an eccentric mass exciter. These simplified load distributions mean that the test loading in some cross sections will be higher than required in order to reach the test load in other cross sections. In this paper the information obtained by the higher test loads is taken into account under the assumption that the test does not lead to failure.

More tests would decrease the statistical uncertainty and could imply a decrease in the partial safety factors leading to a lighter design of the wind turbine blades. Even though full-scale tests of wind turbine blades are time-consuming and expensive the benefits from a lighter design is excessive, since also loads on other parts of the wind turbine are reduced. Besides, the series production of blades implies the possibility that costs of more tests can be paid due to decrease in the use of materials.

In this paper only ultimate loading in the standstill mode and fatigue loading are taken into account. The stochastic models presented for the material properties and uncertainties are based on the work presented in [3] and [4]. The fatigue strength is modelled using the SN-approach in the shape of Constant Life Diagrams and Miner's rule.

In section 2 ultimate loading is first examined by outlining a general load-bearing capacity model for the wind turbine blade and by a numerical example where the partial safety factors are updated based on additional full-scale tests and a simple linear limit state function. In section 3 fatigue loading is considered where a limit state function is arranged based on a numerical simulation of the flapwise bending moment at different mean wind speeds. Subsequently, the partial safety factors are updated based on additional full-scale tests and the limit state function.

2. Ultimate Loading (standstill)
In the following the approach for calculation of the reliability index is outlined, see [5], and it is illustrated by a numerical example how the partial safety factor can be updated based on additional full-scale tests. The following approach is based on a model where the load-bearing capacity of the blade is modelled as a series system of elements, see figure 1. However in real wind turbine blades the single elements are often constructed as a parallel system, which prevents local defectives from dissipating to the entire element (damage tolerant design) and makes the single elements redundant.

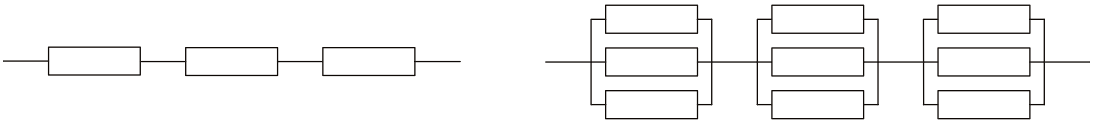

Figure 1: Series and series/parallel system for modelling of wind turbines blades.

In the following it is assumed that a positive correlation exists between the material properties in the single elements of the blade, and a correlation from blade to blade due to common material sources.

Tests with wind turbine blades can be modelled within a framework, where a decreasing number of tests are performed with more complicated structures, see figure 2 and [6]. In this paper the design of the wind turbine blades has been divided into three different levels.

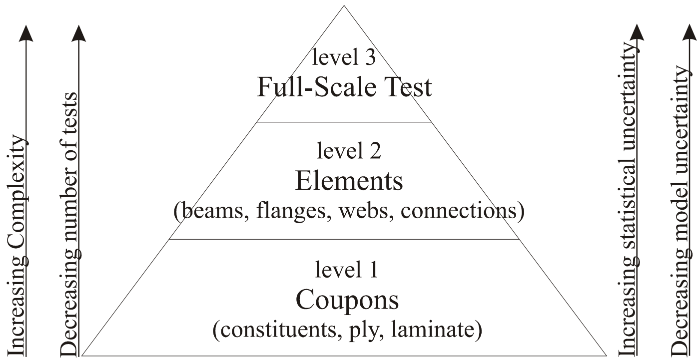

Figure 2: Framework for tests of wind turbine blades, see also [6].

The decreasing number of tests with more complicated structures means that the statistical uncertainty increases at each level of the figure. On the other hand, the model uncertainty on the load-bearing capacity is decreasing because more accurate models are used implicitly accounting for local defects etc. These local defects will differ at each level because the increase in size will introduce new types of defects. In the general case, the load-bearing capacity R of the wind turbine blade is written

$$R = X_R \, R_R \left(\mathbf{X}, \mathbf{P} \right) \tag{1}$$

where X_R is the model uncertainty including statistical uncertainty. R_R is a load-bearing capacity model for instance obtained by a finite element model on basis of which different limit states are calculated with both linear and nonlinear models such as fibre failure analysis and buckling analysis. The load-bearing capacity model depends on the material strength properties given by a vector of stochastic variables $\mathbf{X}$. The vector $\mathbf{P}$ contains deterministic parameters.

At level 1 coupons with the base material are considered and the coupons can in the sense of [7] be considered as a kind of reference volume on micro-scale. Therefore, level 1 contains the physical and statistical uncertainty related to the material properties including the effect from local defectives in the coupons. The physical uncertainty (aleatory uncertainty) cannot be reduced, but the statistical uncertainty (epistemic uncertainty) can be reduced by performing additional tests. The uncertainty related to the material properties is modelled by stochastic variables $\mathbf{X}$ which contain both the physical and statistical uncertainty, but not model uncertainty. $\mathbf{X}$ can be both space and time dependent. The stochastic variables can be determined from tests and prior knowledge from engineering judgement by use of a Bayesian procedure given in e.g. [7] and [8]. The updated material properties from this level are used at the next levels.

At level 2 elements of the blade are considered, which can be considered equivalent to the meso-scale level [7]. The uncertainties related to elements of the blades are mainly related to the material properties, where size effects and local defectives influence the load-bearing capacity of the blade. Even small local defectives will often have a large influence because the element can be regarded as a weakest link model with defects modelling the elements. The model and statistical uncertainty related to the element level X_{elem} are therefore modelled by a Weibull distribution. The uncertainty on the element level will also depend on how good the load-bearing capacity model can predict these local defectives and the size of the element compared to the coupon size. The load-bearing capacity of an element is written

$$R_{element} = X_{elem} R_{elem}\left(\mathbf{X},\mathbf{P}\right) \tag{2}$$

At level 3 full-scale tests with the blade are considered which also can be considered equivalent to the meso-scale level [7]. The model and statistical uncertainties related to the full-scale level are generally the same as for the element level which contains size effects and local defectives. The model and statistical uncertainty related to the full-scale level X_{full} is modelled by a Weibull distribution and the uncertainty is among others dependent on the full-scale size compared to the size of the elements. Therefore, X_{full} models the extra uncertainty from level 2 (element) to level 3 (full-scale). The load-bearing capacity of the full-scale blade is written

$$R_{full-scale} = X_{full} X_{elem} R_{full}\left(\mathbf{X},\mathbf{P}\right) \tag{3}$$

The model and statistical uncertainties X_{elem} and X_{full} related to level 2 and 3 can be calibrated based on tests and prior knowledge by a method similar to the one described in [8] annex D, which is based on Bayesian statistics. It is not taken into account that the full-scale test only captures some of the real load cases.

The above approach is general for all limit states, but in the following only a simple linear limit state is considered for calculating the internal stresses in the blade. This simple method is rather crude and a more refined nonlinear model should be preferred for calculating the internal stresses. However, part of the uncertainty introduced by applying the linear model can be made up by introducing extra uncertainty in the model uncertainties X_{elem} and X_{full}.

Design equation and limit state function (standstill)

The limit state function and the design equation are in the general case written

$$g = R - S \tag{4}$$

$$R_d \geq S_d \tag{5}$$

where R is the load-bearing capacity of the blade and S is the load. Wind turbine blades are primarily exposed to aerodynamic and gravity loads. In the following flapwise bending is considered and only the aerodynamic loading is taken into account. The design equation is written

$$\frac{R_c}{\gamma_m \gamma_n} \geq \gamma_f S_c \tag{6}$$

where R_c and S_c are the characteristic value of the load-bearing capacity and load, respectively. γ_m, γ_n and γ_f are the partial safety factors defined in table 1. The general limit state function for a wind turbine blade in flapwise bending can be formulated according to [3].

$$g = X_R R(X) - X_{dyn} X_{\exp} X_{st} X_{aero} X_{str} X_{sim} S\left(P_w, I\right) \tag{7}$$

where $R(X)$ is the load-bearing capacity model and $S(P_w, I)$ is the load model dependent on the mean wind pressure and the turbulence intensity. For the load the model and statistical uncertainties are divided into their respective components according to [3]. X_{dyn} is the uncertainty related to modelling of the dynamic response for the wind turbine, such as damping ratios and eigenfrequencies. $X_{\exp}$ is the uncertainty related to the modelling of the exposure such as the terrain roughness and the landscape topography. X_{st} is taking the statistical uncertainty related to the limited amount of wind data into account and X_{aero} is related to the uncertainty in assessment of the lift and drag coefficients. X_{str} accounts for the uncertainty related to the computation of stresses from the wind load. The uncertainty X_{sim} accounts for the statistical uncertainty related to the limited number of simulations in order to estimate the extreme load effect.

By inserting the load-bearing capacity R and the load S into the design equation we obtain

$$\frac{\sigma_c}{\gamma_m \gamma_n} \geq \gamma_f c_{\inf} p_{w,c}\left(1 + 2k_p I_c\right) \tag{8}$$

where σ_c is the characteristic material strength and k_p is a peak factor which according to [9] is 3,5. $c_{\inf}$ is an influence factor which is proportional to the section modulus. The limit state function is written

$$g_{full-scale} = X_{full} X_{elem} \Sigma - c_{\inf} P_w \left(1 + 2k_p I \, X_{dyn}\right) X_{\exp} X_{st} X_{aero} X_{str} X_{sim} \tag{9}$$

where Σ is the material strength. A similar limit state function can be arranged for elements of the blades by omitting X_{full}.

Limit state function (full-scale tests)

In full-scale testing the limit state function is written as in formula (4). However, in the full-scale testing the load is applied in a controlled manner and magnitude according to the guidance in [2]. The test load is determined from the characteristic value of the material strength properties multiplied by partial safety factors. The limit state function under full-scale tests is written

$$h_{full-scale} = \gamma_m X_{full} X_{elem} \Sigma - \kappa \gamma_s \gamma_l \sigma_c X_{str} \tag{10}$$

where the partial safety factors γ_s and γ_l are defined in table 1 and κ is modelling the load factor in a selected cross-section. Similarly to (10) a limit state function for test of blade elements can be arranged by omitting X_{full}.

Updating of the probability of failure

The information collected by full-scale tests can be taken into account by updating the probability of failure in the case where the test blade survives the full-scale test. At full-scale level n test blades are taken into account and the updated probability of failure for the blade $P^u_{f,full-scale}$ is written

$$P^u_{f,full-scale} = P\left(g_{full-scale} \le 0 \;\middle|\; \bigcap_{i=1}^{n} h_{full-scale,i} > 0 \right) \tag{11}$$

However, if the wind turbine blade is considered at element level and consisting of m elements capturing the entire blade, the updated probability of failure for the whole blade can be written

$$P^u_{f,full-scale} = P\left(\bigcup_{j=1}^{m} g_{element,j} \le 0 \;\middle|\; \bigcap_{i=1}^{n} \bigcap_{j=1}^{m} h_{element,ij} > 0 \right) \tag{12}$$

As explained previously, the material properties for the blade material $\mathbf{X}$ can vary in both space and time. In order to calculate the updated probability of failure it is necessary to establish this variation in terms of a correlation coefficient function. The correlation coefficient function will primarily depend on how local defectives and material properties are distributed in a wind turbine blade. However such a model is not yet available.

When the updated probability is considered at element level it is necessary to establish a correlation coefficient function for the variation within blades and between blades. At the full-scale level only a function for the variation between blades is necessary because the variation within blades is captured by the stochastic variable X_{full}. However, if the correlation coefficient function is known X_{full} can be calibrated from this and reverse.

In the following the limit state function is considered at full-scale level and it is assumed that the material properties only vary in space and not in time. The correlation of the material properties from blade to blade is given by ρ_B which is assumed to be $\rho_B = 0.50$. The stochastic variables for the model and statistical uncertainties are assumed to be fully correlated.

Partial safety factors and stochastic models

The partial safety factors taken from [2], [6] and [10] are listed in table 1.

Table 1: Partial safety factors, ultimate and fatigue loading.

Name	Description	Ultimate	Fatigue
γ_m	Partial safety factor for blade material	1.2	1.2
γ_n	Partial safety factor for consequences of failure (class 2)	1.0	1.15
γ_f	Partial safety factor for loads, see equation (13)	1.1-1.35	1.0
γ_s	Partial safety factor for blade to blade variation	1.1	1.1
γ_l	Partial safety factor for environmental effects	1.0	1.0
γ_e	Partial safety factor for error in fatigue formulation ($5\cdot10^6$ cycles)	-	1.025

In the 3rd edition of IEC 61400-1 [10] the partial safety factor for loads is a function of the ratio between the response from gravity loading and the characteristic response. In standstill mode the partial safety factor is given by

$$\gamma_f = 1.1 + 0.25\varsigma^2 \qquad \text{where} \qquad \varsigma = \begin{cases} 1 - \left| \dfrac{F_{gravity}}{F_c} \right| & ; \quad |F_{gravity}| \le |F_c| \\ 1 & ; \quad |F_{gravity}| > |F_c| \end{cases} \tag{13}$$

The stochastic models for the loads and material properties taken from [3] and [9] are listed in table 2.

Table 2: Stochastic models for loads and material properties, ultimate loading. Abbreviations: N – Normal distribution, LN – LogNormal distribution, G – Gumbel distribution, W – Weibull distribution, COV – Coefficient of variation, Char – Characteristic value, μ - mean value.

Name	Description	Type	COV	Char.
Σ	Material strength for fiber reinforced polymer	LN	10 %	5 %
P_w	Mean wind pressure	G	23 %	98 %
I	Turbulence intensity	LN	5 %	μ

According to [10], the mean value for the turbulence intensity I is determined to 0,11. The stochastic models for the model and statistical uncertainties taken from [3], [4], [11] and by engineering judgement are listed in table 3.

Table 3: Stochastic models for model and statistical uncertainties, ultimate and fatigue loading.

Name	Description	Category	Type	COV	Char.
Δ	Linear damage accumulation	-	LN	30 %	μ
X_{elem}	Elements	Materials	W	5 %	μ
X_{full}	Full-scale	Materials	W	5 %	μ
X_{dyn}	Structural dynamics	Load effect	LN	5 %	μ
$X_{\exp}$	Exposure	Exposure	LN	20 %	μ
X_{st}	Climate statistics	Exposure	LN	10 %	μ
X_{aero}	Shape factors	Load effect	G	10 %	μ
X_{str}	Stress evaluation	Load effect	LN	3 %	μ
X_{sim}	Simulation statistics	-	N	5 %	μ
X_{RFC}	Rainflow counting	-	LN	2 %	μ

Results

The partial safety factor γ_m as a function of the number of full-scale blade tests is given in figure 3 for different values of the load factor κ. The partial safety factor is determined by calibration of the updated probability failure (11) to the probability of failure for the limit state function in (9). The accumulated probability of failure is $P_f = 1.3\cdot10^{-2}$ corresponding to an accumulated reliability index of β =2.24. The annual reliability index is β =3.12.

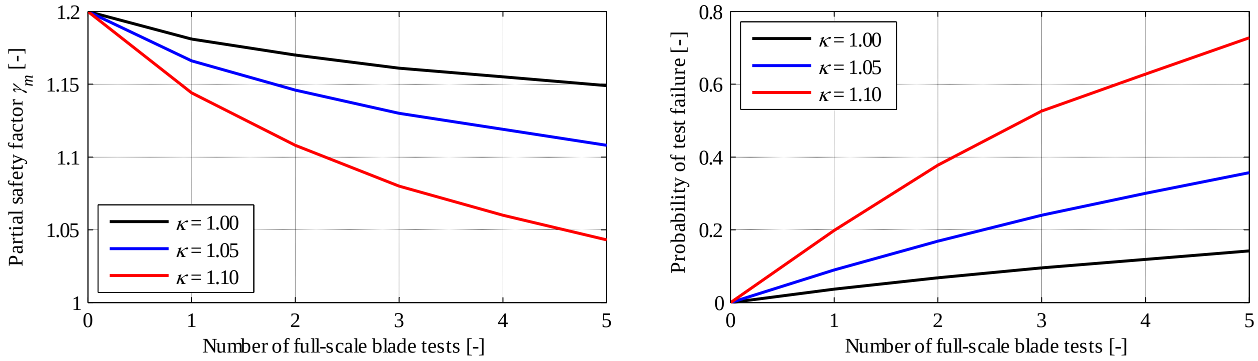

Figure 3: Partial safety factor and probability of test failure dependent on number of full-scale tests and load factor κ.

From the figure it is seen, that the number of full-scale tests has a significant influence on the partial safety factor γ_m. However, the load factor κ regarding the simplified load distribution has a great influence on the partial safety factor under the assumption that the blade survives the full-scale test. As seen from the figure, this assumption is not always fulfilled especially for a high load factor. If a blade fails the test it will lead to a large increase in the partial safety factor even though the blade fails at a higher test load than required. The increase in the partial safety factor will be largest if there is a high correlation between the material properties from blade to blade.

The above-mentioned calculation for the standstill position should also be performed for operational conditions, which can be critical for wind turbines, because the magnitude of the loads is influenced by the control system.

3. Fatigue loading

For fatigue loading the framework used for ultimate loading in figure 2 can also be applied because the uncertainties in the material properties on the higher levels are dependent on size effects and local defectives. In the following the general formulas for fatigue strength calculation are outlined using an SN-approach in the framework of Constant Life Diagrams and Miner's rule. Subsequently the approach for calculation of the reliability index is outlined and it is by a numerical example illustrated how the partial safety factor can be updated based on additional full-scale tests. This example is based on stochastic simulation of the flapwise bending moment at the blade root for twelve different mean wind speeds.

The fatigue approach used in this paper is based on linear damage accumulation given by Miner's rule. A more refined nonlinear damage model could be used which according to [12] gives better results. However, the linear Miner's rule is still the damage model used by the industry and recommended in [6] and [10].

$$D = \sum_k \frac{n_k l}{N_k} \tag{14}$$

where n_k is the number of cycles per year in the stress range σ_k and N_k is the number of stress cycles which the blade can resist in this stress range. l is the lifetime in years. The S-N curve for the blade material can for a given *R*-ratio be approximated by, see [13]

$$\log N_k = \log K - m \log \sigma_k + \varepsilon \tag{15}$$

where m is the slope of the S-N curve and $\log K$ is determining the location of the S-N curve. ε is the residual term. The applied S-N curve is given in terms of stresses but a similar approach could be taken in terms of strains. For materials used in wind turbine blades the mean stress often has a significant influence on the fatigue properties. The effect of the mean stress is often modelled by the *R*-ratio

$$R = \frac{\sigma_{\min}}{\sigma_{\max}} \tag{16}$$

where $\sigma_{\min}$ is the minimum stress and $\sigma_{\max}$ the maximum stress in a fatigue stress cycle. According to the recommendations in [6] a Constant Life Diagram is constructed with five different *R*-ratios, see figure 4. The five *R*-ratios [0.5 0.1 -0.4 -1.0 -2.5] have been chosen based on [14] which recommends five *R*-ratios between 0.5 and -2.0 or 0.7 and -2.0. The S-N curves are determined from the “OptiDat – fatigue of wind turbine materials database” [15] and based on constant amplitude tests with the MD2 lay up and the geometry R0400.

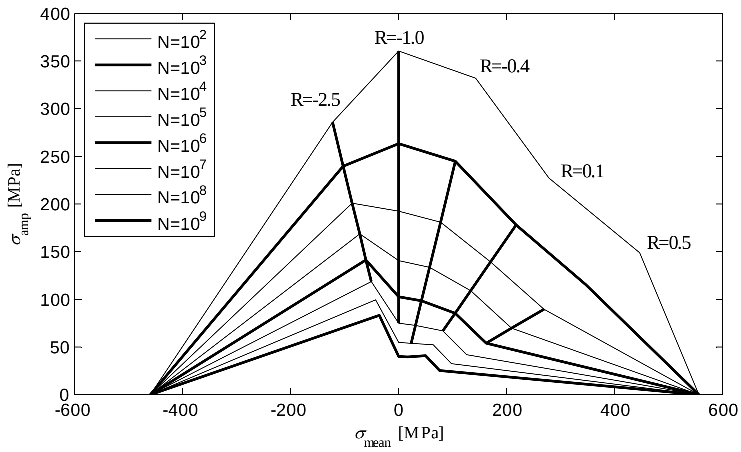

Figure 4: Constant Life Diagram with five different S-N curves for MD2 lay up and geometry R0400.

The Constant Life Diagram in figure 4 is constructed by five S-N curves determined from constant amplitude tests at five different *R*-ratios with coupons of the material. For these constant amplitude data an S-N curve is determined based on (15) and the results are plotted into the Constant Life Diagram for specified values of N. The range of the constant amplitude tests is indicated at each *R*-ratio by a line. Between the different *R*-ratios the fatigue strength is estimated by linear interpolation which is also applied to the ultimate tension and compression strength outside the *R*-ratios.

Real fatigue stress cycles will, however, never be limited to the five *R*-ratios given in figure 4 by means of which interpolation is necessary. In [6] a method is described for transforming fatigue cycles with random *R*-ratios into one of the *R*-ratios given in the Constant Life Diagram (CLD). In the following this method is briefly explained and sketched in figure 5.

Steps in obtaining the expected number of cycles to failure $N_{\exp}$:

- The observed stress cycle P is located in the CLD-diagram as the point with mean stress σ_{mean} and stress amplitude σ_{amp}.
- Draw a line a from the origin of the CLD-diagram through and beyond the point P.
- Identify the two constant life lines closest to P, denoted n_1 and n_2
- Calculate the length a_1 on line a between the two constant life lines n_1 and n_2.
- Calculate the length a_2 on line a between point P and the constant life line n_2.
- Find the *R*-ratio closest to P.
- Calculate the length b_1 between n_1 and n_2.
- Calculate: $b_2 = \frac{b_1 a_2}{a_1}$
- Find the stress amplitude σ_{CLD} corresponding to point Q.
- Obtain the expected number of cycles to failure $N_{\exp}$ using the S-N curve for the given *R*-ratio.

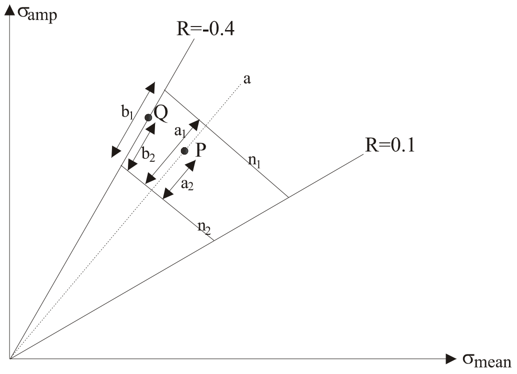

Figure 5: Graphical interpretation of the transformation to known *R*-ratios, see also [6].

Limit state function (operational)

In this paper the limit state function for fatigue is based on a stochastic simulation of the flapwise bending moment at the blade root. The simulations are performed for twelve different mean wind speeds in the range from 3 to 25 m/s. By combining Miner's rule (14) and the SN-approach (15) the limit state function including model uncertainty are written.

$$g_{full-scale} = \Delta - \sum_i p_i l \sum_j \sum_k \frac{n_{ijk}}{K_j 10^{\varepsilon_j}} \left(\frac{X_{dyn} X_{\exp} X_{aero} X_{str} X_{RFC}}{X_{full} X_{elem}} \sigma_{ijk} \right)^{m_j} \tag{17}$$

where index i refers to each of the twelve different mean wind speeds and p_i is the probability that this mean wind speed occurs. The probability p_i is a stochastic variable because the distribution parameters in the Weibull distribution (wind speeds) are modelled by stochastic variables modelling statistical uncertainty. The distribution parameters are assumed having mean value according to IEC class I, coefficient of variation on 5 % and correlated with a correlation coefficient of 0.30 [4]. Index j refers to the different *R*-ratios for the different S-N curves. Index k refers to the different stress range bins. The fatigue stress cycles are determined by rainflow-counting of the flapwise bending moment and the stress cycles are subsequently binned according to mean stress and stress range. These bins correspond to different *R*-ratios which are transformed into the five *R*-ratios given in the Constant Life Diagram, by the method previously described.

The uncertainties in (17) are mainly the same as for ultimate loading. However, the uncertainties X_{st} and X_{sim} in ultimate loading are omitted and two new uncertainties X_{RFC} and Δ are introduced. The uncertainty X_{RFC} models the model uncertainty related to the counting procedure and Δ models the model uncertainty related to Miner's rule for linear damage accumulation, see also [16] and [17].

The uncertainty related to the material properties is at coupon level modelled by the uncertainty in the S-N curve, where also the statistical uncertainty is taken into account. The uncertainty in using the S-N curve from the coupon level on the element and full-scale level (see Figure 2) is modelled by the stochastic variables X_{elem} and X_{full} which are divided the stress range. Because the model uncertainty related to the linear damage accumulation is covered by Δ, X_{elem} and X_{full} only covers the size effects and local defectives from which fatigue cracks often initiate.

Design equation (operational)

The design equation for fatigue loading is used to calibrate the section modulus. According to [6] and [10], the design equation is written.

$$D = \sum_i p_i l \sum_j \sum_k \frac{n_{ijk}}{K_{c,j}} \left(\gamma_m \gamma_n \gamma_f \sigma_{ijk} \right)^{m_j} \leq 1 \tag{18}$$

where subscript *c* is used for characteristic value and D is the damage which equals one when failure occurs. The characteristic value for the material properties is determined according to [10] with a 95 % survival probability with a confidence level of 95 %. The partial safety factors γ_m, γ_n and γ_f are defined in table 1 and the stochastic variables are defined in table 3.

Limit state function (full-scale tests)

Fatigue full-scale testing of wind turbine blades is performed by applying a fatigue damage equivalent to the fatigue damage caused by the design load. In this paper is it assumed that the fatigue test loading is performed by 5·10[6] cycles at the *R*-ratio which is most significant for the rated wind speed. The limit state function for full-scale testing is written, see [10].

$$h_{full-scale} = \Delta - \frac{n_{eq}}{K_j 10^{\varepsilon_j}} \left(\kappa \frac{X_{str}}{X_{full} X_{elem}} \gamma_n \gamma_f \gamma_s \gamma_e \gamma_l \, \sigma_{eq} \right)^{m_j} \tag{19}$$

where the partial safety factors γ_s, γ_e and γ_l are defined in table 1 and the partial safety factor γ_m is omitted according to [10]. In the following it is assumed that the test is characterized by $R = 0.1$.

Updating of the probability of failure

The information collected by full-scale tests can be taken into account by updating the probability of failure for the case where the test blade survives the full-scale test. At full-scale level n test blades are taken into account and the updated probability of failure for the blade $P^u_{f,\,full-scale}$ is written

$$P^u_{f,\,full-scale} = P\left(g_{full-scale} \le 0 \,\middle|\, \bigcap_{i=1}^{n} h_{full-scale,i} > 0 \right) \tag{20}$$

The material properties for fatigue loading are given by the parameters in the S-N curve which are m, K and ε, where m is deterministic. The stochastic variable for the residual term ε models the physical and model uncertainty related to the S-N curve. The statistical uncertainty is modelled by the stochastic variables K and the stochastic variables σ_ε which is the standard deviation of the residual term ε.

As explained for ultimate loading the material properties can vary in space and time also in fatigue loading. In the following the same correlations as for ultimate loading are assumed.

Results

The partial safety factor γ_m as a function of the number of full-scale blade tests is given in figure 6 for different values of the load factor κ. The partial safety factor is determined by calibration of the updated probability of failure (20) to the probability of failure for the limit state function in (17). The accumulated probability of failure is P_f = 1.7·10[-2] corresponding to an accumulated reliability index of β =2.11. The annual reliability index in year 20 is β =3.10.

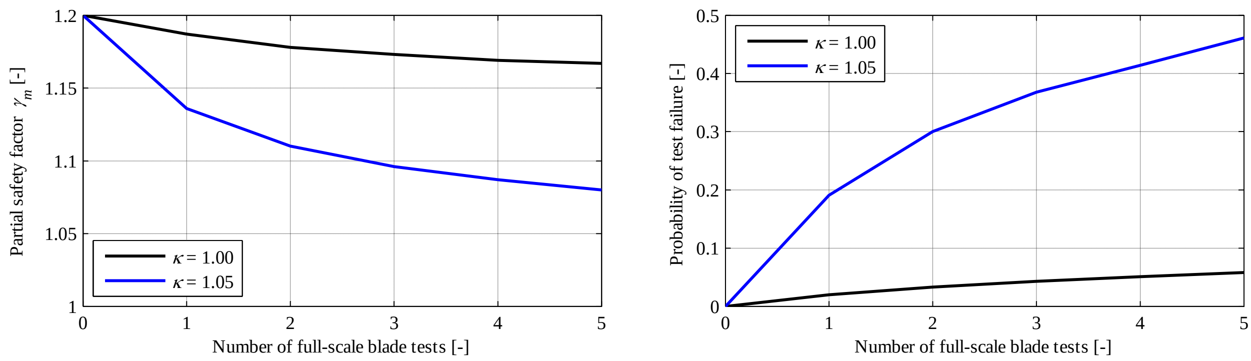

Figure 6: Partial safety factor and probability of test failure dependent on number of full-scale tests and load factor κ.

The result in figure 6 shows the same trend as in figure 3 for ultimate loading, given that the partial safety factor γ_m decreases when additional full-scale tests is performed. However, the load factor κ has a more significant influence in fatigue loading.

4. Conclusion

A probabilistic approach is described for updating the material partial safety factor γ_m in ultimate and fatigue loading when additional information from full-scale tests is taken into account. For both load cases additional full-scale tests will lead to a decrease in the partial safety factor. A much more significant influence on the partial safety factor is seen for the load factor κ, where even a small increase in the test load leads to a significant decrease in the partial safety factor based on the assumption that the blades survive the tests. This extra load factor is often already available because of the simplified load distribution under testing. For higher test loads the influence from additional full-scale tests is also more significant.

The updated partial safety factors are based on the assumption that all blades survive the test. However, if a blade fails it will lead to a significant increase in the partial safety factor, which will be conditional on the load under which the blade failed and the correlation between the material properties from blade to blade.

Acknowledgement

The work presented in this paper is part of the projects 'Probabilistic design of wind turbines' supported by the Danish Research Agency, grant no. 2104-05-0075 and 'Improvement of methods for fatigue assessment' supported by the Danish Energy Authority, EFP2007 grant no. 33033-0077. The financial support is greatly appreciated. Furthermore, Jakob Wedel-Heinen (Det Norske Veritas) is acknowledged for his comments and constructive discussions.

References

[1] IEC WT 01. System for Conformity Testing and Certification of Wind Turbines (Rules and procedures). 1st edition. 2001.
[2] IEC 61400-23. Wind turbine generator systems - Part 23: Full-scale structural testing of rotor blades. 2001.
[3] Tarp-Johansen NJ, Madsen PH, Frandsen S. Partial Safety Factors for Extreme Load Effects. Risø National Laboratory, Roskilde, Denmark; 2002. Report No.: Risø-R-1319(EN).
[4] Tarp-Johansen NJ. Examples of Fatigue Lifetime and Reliability Evaluation of Larger Wind Turbine Components. Risø National Laboratory, Roskilde, Denmark; 2003. Report No.: Risø-R-1418(EN).
[5] Madsen HO, Krenk S, Lind NC. Methods of Structural Safety. Dover Publications, Inc.; 2006. ISBN 0-486-44597-6.
[6] Det Norske Veritas (DNV). Design and Manufacture of Wind Turbine Blades, Offshore and Onshore Wind Turbines. 1st edition. 2006.
[7] Joint Committee on Structural Safety (JCSS). Probabilistic Model Code. 2001. www.jcss.ethz.ch
[8] EN 1990. Eurocode - Basis of structural design. 2002.
[9] EN 1991-1-4. Eurocode - Wind actions. 2005.
[10] IEC 61400-1. Wind turbines - Part1: Design requirements. 3rd edition. 2005.
[11] Sorensen JD, Tarp-Johansen NJ. Reliability-based optimization and optimal reliability level of offshore wind turbines. International Journal of Offshore and Polar Engineering 2005 Jun;15(2):141-6.
[12] Sutherland HJ, Mandell JF. Effect of mean stress on the damage of wind turbine blades. Journal of Solar Energy Engineering-Transactions of the Asme 2004 Nov;126(4):1041-9.
[13] Ronold KO, Wedel-Heinen J, Christensen CJ. Reliability-based fatigue design of wind-turbine rotor blades. Engineering Structures 1999 Dec;21(12):1101-14.
[14] Sutherland HJ, Mandell JF. Optimized constant-life diagram for the analysis of fiberglass composites used in wind turbine blades. Journal of Solar Energy Engineering-Transactions of the Asme 2005 Nov;127(4):563-9.
[15] OPTIMAT BLADES. [July 20th, 2006]. 2006. http://www.wmc.nl/.
[16] Veldkamp HF. Chances in Wind Energy - A Probabilistic Approach to Wind Turbine Fatigue Design [PhD-thesis] Delft University of Technology; 2006.
[17] Det Norske Veritas (DNV). Fatigue Design of Offshore Steel Structures. 1st edition. 2005.